On construction of harmonic maps of spatial domains by the block analytical-numerical method

© Dmitrij B.Volkov-Bogorodsky

Institute of Applied Mechanic of Russian Academy Science,
Leninskij prospect, 32-A, Moscow, 117334 Russia

Tel.: (095)938-51-15, fax: (095)938-07-11,
mailto: dvb@tesis.com.ru

The work is devoted to construction of harmonic mappings of spatial domains onto canonical ones in parametric space. This problem has great practical interest, because it provides reliable method for mesh generation in spatial domains. Construction of harmonic maps is realized by block analytical-numerical method, which is based on decomposition of initial complex-shaped region onto simple sub-domains (blocks) and on approximation of solution in every block by a series of special functions having good approximation properties and accurately satisfying the problem operator. Singular functions can be used near boundary edges, which allows to describe harmonic mapping behavior near angle elements of boundary accurately. The block analytical-numerical method represents solution in analytical form, which is convenient for fast reconstruction of the corresponding harmonic meshes. Numerical evidences suggest that the presented technique is highly competitive practical method for constructing harmonic maps and meshes.

1. Harmonic mapping

We consider the harmonic mapping from any region $G \subset \mathrm{R}^3$ to the canonical region in parameter space $\vec{\xi} = \{\xi_1,\ \xi_2,\ \xi_3\}$:

$$\triangle\ \vec{\xi}(P) = 0, \qquad P \in G. \tag{1}$$

Such mapping $\vec{\xi} = \vec{\xi}(P)$, described in (1), is widely used for constructing of three-dimensional and surface grids in plane and spatial domains [1, 2].

The following regions can be regarded as canonical: unit box $\mathcal{P} = \{\vec{\xi} : 0 < \xi_k < 1,\ \ k = 1, 2, 3\}$, unit ball $\mathcal{B} = \{\vec{\xi} : 0 \le (\xi_1^2 + \xi_2^2 + \xi_3^2)^{1/2} < 1\}$, plain layer $\mathcal{H}_1 = \{\vec{\xi} : 0 < \xi_1 < 1\}$, cylindrical layer $\mathcal{C}_r = \{\vec{\xi} : r < (\xi_1^2 + \xi_2^2)^{1/2} < 1\}$ or spherical layer $\mathcal{B}_r = \{\vec{\xi} : r < (\xi_1^2 + \xi_2^2 + \xi_3^2)^{1/2} < 1\}$ (for doubly-connected regions topologically equivalent to cylindrical or spherical layer).

The unit box $\mathcal{P}$ is commonly used as an instance of the canonical region; in this case it is easy to introduce curvilinear coordinates in the domain G: the coordinates are the result of harmonic mapping $\vec{\xi}(P)$ of points $P \in G$. The coordinate surfaces $\{\xi_k = 0\}$ and $\{\xi_k = 1\}$ will lie on the boundary of the region ∂G. Also in this case the hexahedral grid is easily introduced as the set of coordinate surfaces $\{\xi_k = const\}$. But the coordinates can be computed as described above only in the case of simply connected domains.

We would like to take a more wide look on the problem, when not only $\mathcal{P}$ can be chosen as an instance of the canonical region in the parameter space $\vec{\xi}$, but also $\mathcal{B}$, $\mathcal{H}_1$, $\mathcal{C}_r$ or $\mathcal{B}_r$. This case is interesting because it can be used for doubly-connected regions. The grid in G is introduced by applying the harmonic mapping to the grid already constructed for $\mathcal{B}$, $\mathcal{H}_1$, $\mathcal{C}_r$ or $\mathcal{B}_r$.

The harmonic mapping (1) is defined uniquely if there is a correspondance between the original and canonical domain boundaries, which means that the boundary condition of type one is specified for the equation (1):

$$\vec{\xi}(P') = \vec{h}(P'), \qquad P' \in \partial G. \tag{2}$$

In some cases this correspondance should satisfy additional conditions. The mapping from not simply connected domains, which are topologically equivalent to cylindrical layer, onto the plane layer $\mathcal{H}_1$ is an example where the additional conditions can be introduced.

This paper describes the application of the block analytic-numerical method for the construction of harmonic mapping $\vec{\xi}(P)$, i.e. for solving the problem (1), (2). This method has been developed for a long time and it is applied in boundary value problems of mathematical physics [3-7]. The main feature of the method is the ability to represent the solution as the series of special functions which have good aproximation properties and take into account the geometry singularities of the region boundary that is very important when constructing non-degenerate grids.

The harmonic mapping is defined by the boundary conditions (2) which can be specified in different ways for the same canonical domain. It is of great interest for us to explore the influence of the singular elements of the original region boundary on the mapping and also to study the properties of harmonic mapping around singular elements which influence the resulting grid.

2. System of basis functions

We consider a common solution of Laplace equation (1) (which is a special

case of that for Helmholz equation, see [7]):

$$\Phi(P) = \Phi(w, \overline{w}, z) = \sum_{p=0}^{\infty} (-1)^p \frac{w^{\mu+p}\, \overline{w}^p}{4^p\, (\mu+1)_p\, p!}\, U^{(2p)}(z); \qquad (3)$$

the point $P = (w, \overline{w}, z) \in G$ is represented in the complex form with the variables $w = x+iy$, $\overline{w} = x-iy$, $(a)_p = a\,(a+1)\,\ldots\,(a+p-1)$ is Pokhammer symbol [8], μ is the real parameter, $U(z)$ is any real function of the variable z. Let us represent Laplace operator in complex form with the variables w, $\overline{w}$ and z and put formal series (3) into equation (1), after differentiating and collecting members with equal derivatives $U^{(2p)}$ we obtain identity. The representation (3) uniformly converges in confined domain $G \subset \{A < z < B\}$ and introduce solution of equaion (1) when $|U^{(p)}(z)| \le M^p < \infty$ for any p.

The two factors influence on the common solution (3) – real parameter μ defining the oscillation of the function in the plane $\{z = const\}$ and plane function $U(z)$ which defines the behaviour of solution (3) along the axis z, i.e. $\Phi(P) \Longleftrightarrow \{\mu, U(z)\}$; a lot of known solutions of equation (1) which are found by the method of separation of variables in different orthogonal systems can be represented in the form (3).

For example, the power function $U(z) = z^{\nu-\mu}$ corresponds to separated variables system for the Laplace operator represented in spherical coordinates $P = (\rho,\, \varphi,\, \theta)$. This function can be represented in the form (3) as follows:

$$\Phi(P) = \Phi_\nu^\mu(\rho,\, \varphi,\, \theta) = A_\mu\, \rho^\nu\, e^{i\mu\varphi}\, \mathrm{P}_\nu^{-\mu}(\cos\,\theta) \Longleftrightarrow \left\{\mu, z^{\nu-\mu}\right\}. \qquad (4)$$

The exponential function $U(z) = e^z$ or $U(z) = e^{iz}$ in the representation (3) correspond to the separated variables system for Laplas operator represented in cylindrical coordinates $P = (r,\, \varphi,\, z)$:

$$\Phi(P) = A_\mu\, J_\mu(r)\, e^{i\mu\varphi}\, e^z \Longleftrightarrow \left\{\mu, e^z\right\},\ A_\mu\, I_\mu(r)\, e^{i\mu\varphi}\, e^{iz} \Longleftrightarrow \left\{\mu, e^{iz}\right\}. \quad (5)$$

Here $\mathrm{P}_\nu^{-\mu}(t)$ are Legendre functions of the first type (see [8]) on the cutting, $J_\mu(t)$ are Bessel functions of the first type, $I_\mu(t)$ are modifying Bessel functions, $A_\mu = 2^\mu\, \Gamma(\mu+1)$ where $\Gamma(t)$ is gamma-function of Euler. The representations (4), (5) can be directly examined, if we constitute in (3) formulas $w = re^{i\varphi}$, $\overline{w} = re^{-i\varphi}$, $r = \rho \sin\theta$, $z = \rho\cos\theta$ and use definition of Legendre and Bessel functions [8] by a series.

Let us point out that two functional subsystems, for $\mu = 0$ and for

$U(z) \equiv 1$, can be naturally separated out of (3). They are used for the solution of axis-symmetric and plane problems. The second subsystem is the system of complex powers, i.e. $w^\mu \Longleftrightarrow \{\mu, 1\}$.

In some sense system (4) can be regarded as the simplest functional system extracted from representation (3). The block method for problems (1), (2) solution is based on this system (4); when ν and μ are integers the system (4) becomes a system of (complex) spherical functions (see [9, 10]) up to the multiplier A_μ. We know that these functions form the complete system in L_2-norm on the surface of any ball with the center in the origin of coordinate system.

If we identify the function $\Phi(P)$, defined by the series (3), by its symbol $\{\mu, U(z)\}$, then differential features of functions $\Phi(P) \Longleftrightarrow \{\mu, U(z)\}$ derived from the definition of (3) are the following:

$$\frac{\partial}{\partial z}\Big\{\mu,\, U\Big\} = \Big\{\mu,\, U'\Big\}, \quad \frac{\partial}{\partial w}\Big\{\mu,\, U\Big\} = \mu\,\Big\{\mu-1,\, U\Big\}, \quad \mu \neq 0; \tag{6}$$

$$\frac{\partial}{\partial \overline{w}}\Big\{\mu,\, U\Big\} = -\frac{\Big\{\mu+1,\, U''\Big\}}{4\,(\mu+1)}. \tag{7}$$

Relations (6) are checked directly by differentiating of (3); relation (7) is derived from the complex representation of Laplace operator and (6). When $\mu = 0$ functions (3) are real. The formula (6), which is used for differentiating of (3) when $\mu = 0$, is following from (7) after applying complex conjugation.

The corresponding differential relations for Φ^μ_ν are derived from (4) after placing the function $U(z) = z^{\nu-\mu}$ into (6) and (7):

$$\frac{\partial\,\Phi^\mu_\nu}{\partial\, z} = (\nu-\mu)\,\Phi^\mu_{\nu-1}, \quad \frac{\partial\,\Phi^\mu_\nu}{\partial\, w} = \mu\,\Phi^{\mu-1}_{\nu-1}, \quad \mu \neq 0; \tag{8}$$

$$\frac{\partial\,\Phi^\mu_\nu}{\partial\,\overline{w}} = -\frac{(\nu-\mu)(\nu-\mu-1)}{4\,(\mu+1)}\,\Phi^{\mu+1}_{\nu-1}. \tag{9}$$

As we can see, the derivatives on z and on w for the functions (4) are the same as for the power function. Apart from (8) and (9) the functions (4) satisfy recurrent relations (which are checked by the recurrent relations between Legendre functions [8]):

$$\Phi^\mu_\nu = \frac{2\nu-1}{\nu+\mu}\,z\,\Phi^\mu_{\nu-1} - \frac{\nu-\mu-1}{\nu+\mu}\,(w\overline{w}+z^2)\,\Phi^\mu_{\nu-2}; \quad \Phi^\mu_\mu = w\,\Phi^{\mu-1}_{\mu-1}. \tag{10}$$

Relations (8) – (10) happen to be valuable when implementing the block analytic-numerical method for solution of problems (1) and (2).

3. Theorem on representation of harmonic mapping

When $\nu = n \geq 0$ and $\mu = m \geq 0$ are integers, functions Φ_ν^μ become homogeneous harmonic polynomials (or spherical functions), which form the complete orthogonal system in space L_2 on the surface of any ball with the center in the origin of coordinate system [9, 10]. Relations (9) allow to decrease the power of these functions by differentiating. According to (3), they can be represented in the form which allow to create the analogue of these functions in the surface R^3 with power w^μ. Due to these features it becomes possible to build the Taylor series for 3D Laplace equation solutions, and to represent the harmonic mapping (1), (2) as the infinite series of functions Φ_ν^μ.

Theorem 1 (on convergence of 3D Taylor series). *Let point $P_0 \in G$ and $\mathcal{B}(P_0)$ be a ball of some radius with center in point P_0, which totally lies in domain G. Then harmonic mapping $\vec{\xi}(P)$, defining by (1), (2), may be represented in ball $\mathcal{B}(P_0)$ as a convergent series (when ν, μ are integer):*

$$\vec{\xi}(P) = \vec{\xi}(P_0) + \mathrm{Re} \sum_{\nu=1}^{\infty} \sum_{\mu=0}^{\nu} \vec{A}_{\nu\mu}\, \Phi_\nu^\mu (P - P_0), \tag{11}$$

when coefficients $\vec{A}_{\nu\mu} = \{A_{\nu\mu}^{(1)},\, A_{\nu\mu}^{(2)},\, A_{\nu\mu}^{(3)}\}$ are calculated by differential formulas

$$\vec{A}_{\nu\mu} = \frac{2 - \delta_\mu^0}{\mu\,!\,(\nu - \mu)\,!} \left. \frac{\partial^\nu \vec{\xi}(P)}{\partial w^\mu\, \partial z^{\nu-\mu}} \right|_{P=P_0}, \tag{12}$$

here δ_μ^0 is Kroneker symbol, $\delta_\mu^0 = 1$ when $\mu = 0$, $\delta_\mu^0 = 0$ when $\mu \neq 0$.

Let us point out that relations (8), (9) allow to calculate easily any differential combinations of functions (4) and thus they become valuable for algorithmic implementation of (11). The block analytic-numeric method for problem (1), (2) is based on formula (11) (for more information see [7]).

4. Singular functions

Let us consider spatial bihedral corner $G = \{P = (r,\, \varphi,\, z) :\ 0 < \varphi < \pi\beta\}$ and its harmonic mapping on the half space $\mathcal{H} = \{\vec{\xi} :\ \xi_2 > 0\}$. We set up

correspondence between boundaries of domains G and $\mathcal{H}$ in the form:

$$\xi_1(P) = \mathrm{Im}\,(x+iy)\,e^{-i\pi\beta/2}, \qquad \xi_2(P) = 0, \qquad \xi_3(P) = z. \tag{13}$$

This correspondence sets uniform grid on the both borders of ∂G. Note, that formula (13) introduces some degenerate harmonic mapping of whole space. We must entroduce into ξ_2 nonzero harmonic function, which admits zero value on the surface ∂G, in order to define the true mapping.

Such functions are well-known in complex analysis of one variable; for example, they were used as a basis for development of analytical-numerical method for the plane Poisson equation solution, and they were explored and widely used in [3-6]. These functions conform to the common representation (3) when $\mu = m/\beta$. Relation $\mathrm{Im}\,\Phi_\nu^{m/\beta} = 0$ is derived from (4) when $\varphi = 0$ and $\varphi = \pi\beta$, i.e. when on the surface of the bihedron.

So, the harmonic mapping of the bihedral corner G onto the half-space is described by the following:

$$\xi_1(P) = \mathrm{Im}\,(x+iy)\,e^{-i\pi\beta/2}, \quad \xi_2(P) = \mathrm{Im}\;\Phi_{1/\beta}^{1/\beta}(P), \quad \xi_3(P) = z. \tag{14}$$

Function (4) is used in (14) above with $\nu = 1/\beta$ and $\mu = 1/\beta$. On the fig. 1 is shown the harmonic grid of the mapping (12) around the corner (left

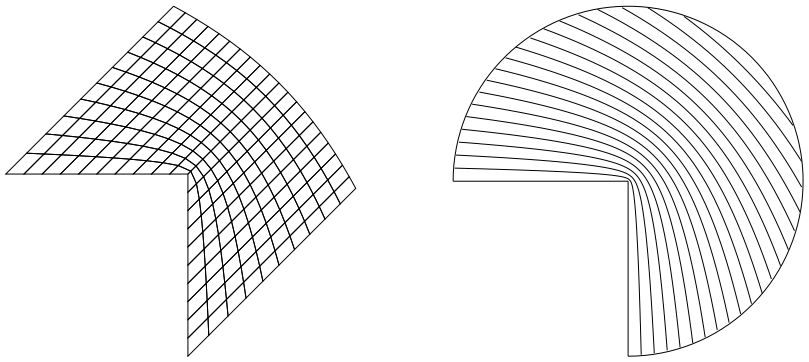

Figure 1: Harmonic mapping of the bihedral corner (in section $z = 0$)

picture) and the levels of the function $\xi_2(P) = \mathrm{Im}\;\Phi_{1/\beta}^{1/\beta}(P)$ in the section $z = 0$ (axis z is directed towards the figure plane); the grid is uniform along the axis z. On the right picture we see the effect of level lines concentration

around the vertex of the corner. The effect is due to the existence of the function Φ_ν^μ in the mapping when $\mu < 1$ ($\mu = 1/\beta = 2/3 < 1$ because $\beta = 3/2$). From the formula (3) follows that the derivative in direction r is approaching the infinity when $\mu < 1$:

$$\frac{\partial \Phi_\nu^\mu}{\partial r} \sim r^{\mu-1}\, e^{i\mu\varphi} z^{\nu-\mu} \to \infty, \quad r \to 0,$$

i.e. functions Φ_ν^μ are singular when $\mu < 1$. This is the reason for the isolines concentration effect. But in this case the effect does not result in the appearance of the degenerate elements in the grid.

Under conditions (13) the mapping from G onto $\mathcal{H}$ is not unique, the singular function Φ_ν^μ with some coefficient can also be included into the equation for coordinate $\xi_1(P)$:

$$\xi_1 = \mathrm{Im}\left\{(x+iy)\, e^{-i\pi\beta/2} + A\,\Phi_{1/\beta}^{1/\beta}\right\}, \quad \xi_2 = \mathrm{Im}\ \Phi_{1/\beta}^{1/\beta}, \quad \xi_3 = z. \qquad (15)$$

Formulas (15) also give the mapping of the bihedral corner onto $\mathcal{H}$, however the effect of isolines concentration will appear for the coordinate $\xi_1(P)$ as well. On the fig. 2 we can see the iso-levels of $\xi_1(P)$ in section $z = 0$ with $A = -1$, $A = 0$ and $A = 1$. As we see, when $A = 0$ the angle between

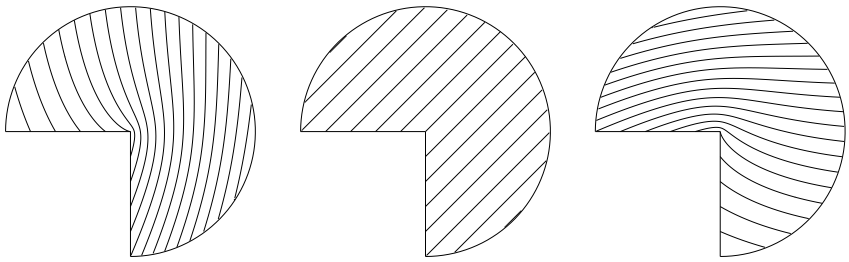

Figure 2: Levels of coordinate $\xi_1(P)$ around bihedral corner (in section $z = 0$)

the line $\xi_1(P) = 0$ and the border is equal to 45°, and when $A \neq 0$ it is equal to zero (on the left and on the right of the figure). The lines become more concentrated when approaching the corner. This effect happens for any value of coefficient A, only the sign of the coefficient is important. This behaviour of the function $\xi_1(P)$ can result in appearance of degenerate elements in harmonic grid.

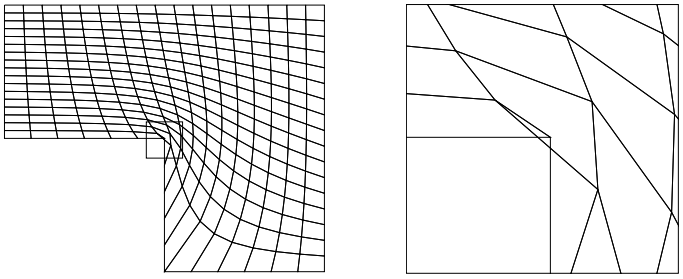

Figure 3: Grid degeneration around the vertex of the corner

On the fig. 3 on the left the harmonic grid in the plane domain is drawn, it contains the re-entrant corner. The zone around the corner is shown on the right, it contains the degenerate quadrangle. The calculation was made by the block analytic-numeric method based on functions (4) when $\nu = \mu = m \geq 0$ was integer.

The bihedral corner with two plane boundaries is one of the most frequently encountered geometrical elements of spatial regions. For example, test region G, which is subtraction $\mathcal{P}_0 \backslash \mathcal{P}_1$ of two boxes where $\mathcal{P}_0 = \{P : 0 < x < 2, 0 < y, z < 1\}$ and $\mathcal{P}_1 = \{P : 0 < x < 1, 0 < y, z < 1/2\}$ is shown on fig. 4. In the neighborhood of the point $M = \{1, 1/2, 1/2\}$ lie

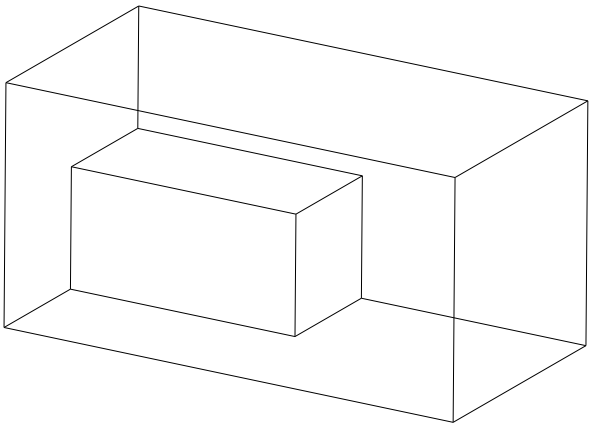

Figure 4: Example of domain for harmonic mapping calculation

three bihedral corners, which constitute the spatial trihedral corner – more complicated geometrical element. In the neighborhood of each bihedron (but out of neighborhood of the point M) harmonic mapping is described by $\{\Phi^{\mu}_{\mu+n}\}$, $\mu = m/\beta$, $\beta = 3/2$. They can contain singular functions $\{\Phi^{\mu}_{\nu}\}$, $\mu < 1$.

The completness of the system $\{\Phi^{\mu}_{\mu+n}\}$, $\mu = m/\beta$, on the surface of cylindrical sector $\mathcal{C}_{r,\beta}(L) = \{P : \sqrt{x^2+y^2} < r,\ 0 < \varphi < \pi\beta,\ 0 < z < L\}$ can be proved according to representation (3) and formulas (4) and (5).

Theorem 2 (on completness of function system). *Let $\mathcal{C}_{r,\beta}(L)$ be cylindrical sector by radius r, length L and angle $\pi\beta$, and let there exists domain $G \supset \mathcal{C}_{r,\beta}(L)$ such, that $S_1(\varepsilon) = \{P : \sqrt{x^2+y^2} < r,\ \varphi = 0,\ \varphi = \pi\beta,\ -\varepsilon < z < L+\varepsilon\} \subset \partial G$, $\varepsilon > 0$. Then system of functions $\{\Phi^{\mu}_{\mu+n}\}$, $\mu = m/\beta$, $n, m \geq 0$, is complete in space $L_2(\partial\mathcal{C}_{r,\beta}(L))$ of harmonic in G functions, which admit zero value on the surface $S_1(\varepsilon)$.*

5. General scheme of the least squares method on multi-block structure

We consider the coverage of the original region by the finite block system $\{\mathcal{B}_k\}$, $G = \cup\mathcal{B}_k$, each of which is the simple-connected subregion of G. Let the blocks $\mathcal{B}_k$ and $\mathcal{B}_l$ be called neighbouring when $\mathcal{B}_k \cap \mathcal{B}_l \neq \emptyset$ and let us assume that the intersection of the neighbouring blocks is $\mathcal{B}_{kl} = \mathcal{B}_k \cap \mathcal{B}_l \subset G$.

Let us divide the boundary of the block $\mathcal{B}_k$ on two parts, $\partial\mathcal{B}_k = S_0^{(k)} \cup S_1^{(k)}$, where $S_1^{(k)}$ is the part of the given region border, on which the boundary condition (2) is fulfilled, and $S_0^{(k)}$ is a part of the block boundary which intersects with the neighbouring blocks. According to region coverage conditions the last part can be represented as the union $S_0^{(k)} = \cup S_{kl}$, $S_{kl} = \partial\mathcal{B}_k \cap \overline{\mathcal{B}_l}$, of all parts of the block $\mathcal{B}_k$ boundary, included into all neighbouring blocks $\mathcal{B}_l$. So, the boundary of each block can be represented as follows:

$$\partial\mathcal{B}_k = S_k = \cup S_{kl} \cup S_1^{(k)}, \quad l \in \{l : \mathcal{B}_k \cap \mathcal{B}_l \neq \emptyset\}. \tag{16}$$

On the fig. 5 there is an example of the region $G = \mathcal{P}_0 \backslash \mathcal{P}_1$ coverage by the spherical blocks $\mathcal{B}_k$, constructed by intersection of the balls $\mathcal{B}(P_0)$ of any radius and the region G itself. All region is covered by 14 blocks, only 5 of them (for keeping the figure clear) are drawn on the fig. 5.

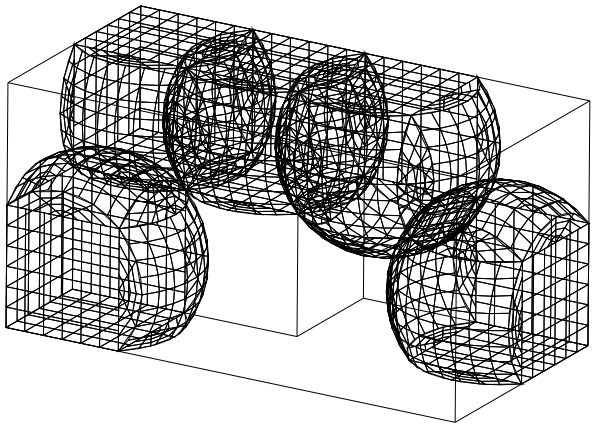

Figure 5: Subdivision on spherical blocks of 3D domain

We introduce a local mapping $\vec{\xi}^{(k)}(P)$ in each block $\mathcal{B}_k$ and approximate it by finite series according to theorem 1

$$\vec{\xi}^{(k)}(P) = \mathrm{Re} \sum_{\nu=0}^{N_k} \sum_{\mu=0}^{\nu} \vec{\mathrm{A}}_{\nu\mu}^{(k)} \, \Phi_{\nu}^{\mu}(P - P_0). \tag{17}$$

For a number of blocks (we call them singular blocks) the harmonic mapping near the edges of bihedral corners can be described with the help of functions $\{\Phi_{\mu+n}^{\mu}\}$, $\mu = m/\beta$. In that case they should satisfy additional conditions: 1) in some local coordinate system $\tilde{P} = Q(P - P_0)$, where Q is the orthogonal mapping from class $SO(3)$, region $\mathcal{B}_k$ takes the shape of cylindrical section $\mathcal{C}_{r,\beta}(L)$; 2) surface $S_1^{(k)}$ of the block boundary becomes surface S_1 of bihedral corner $\mathcal{C}_{r,\beta}(L)$ in local coordinate system.

We approximate the local mapping $\vec{\xi}^{(k)}(P)$ by the finite series with real coefficients for each singular block $\mathcal{B}_k$ according to theorem 2:

$$\vec{\xi}^{(k)}(P) = \vec{\xi}_0^{(k)}(P) + \sum_{n=0}^{N_k} \sum_{m=0}^{M_k} \vec{\mathrm{A}}_{nm}^{(k)} \, \mathrm{Im}\, \Phi_{m/\beta+n}^{m/\beta}(\tilde{P}), \tag{18}$$

where $\vec{\xi}_0^{(k)}(P)$ is a solution of equation (1) which takes a boundary value (2) on the surface $S_1^{(k)}$.

Local solutions are stitched together with the method of the least squares [11] in L_2-norm, that accounts for deflection of the boundary value with respect to the given function, and difference coordinate functions in the adjacent blocks interlace area:

$$\left\|\vec{\xi}^{(k)}(P') - \vec{h}(P')\right\|^2_{S_1^{(k)}} + \left\|\vec{\xi}^{(k)}(P') - \vec{\xi}^{(l)}(P')\right\|^2_{S_{kl}} \to \min\,. \qquad (19)$$

Realization of such approach of respecting the boundary conditions together with stitching of local solutioins in blocks results in the need to solve the system of linear equations, having block structure:

$$A_k\, X_k + \sum_l T_{kl}\, X_l = H_k, \quad k = 1, 2, \ldots N_{sm}, \qquad (20)$$

where A_k is the Gram matrix of the system (4) used for k-th block, X_k is the vector of unknown coefficients in the representation (17), (18), T_{kl} are matrices, that provide for stitching of the local block solutions, H_k is the vector of boundary conditions in the block, N_{sm} – the number of blocks in the structure. After reordering (20) the block system corresponds to the sparse banded structure, with diagonal blocks dominating the matrices T_{kl}. The system of equations (20) has good algebraic properties, and different block analogues of direct and iterative methods of linear equation systems solution can be applied for its solution.

6. Harmonic mapping of domain $G = \mathcal{P}_0 \backslash \mathcal{P}_1$

We apply the block analytic-numeral method described in part 5 for constructing the harmonic mapping of the reqion G depicted on fig. 4. We would like make such a mapping on $\mathcal{P}$ for which the lower part of the area containing the lug is mapped on the lower side of the parametrical cube $\mathcal{P}$. Let us determine the correspondence between the boundaries of regions G and $\mathcal{P}$; on sides $\{x = 2\}$, $\{y = 1\}$ and $\{z = 1\}$ let set the relations:

$$\xi_1(P) = \frac{x}{2}, \qquad \xi_2(P) = y, \qquad \xi_3(P) = z, \qquad (21)$$

and on the lower surface containing the lug:

$$\xi_1(P) = \frac{x}{2}\,(1 - y), \qquad \xi_2(P) = 0, \qquad \xi_3(P) = z\,(1 - y). \qquad (22)$$

On other sides $\{x = 0\}$, $\{z = 0\}$ let us find the mapping between the plane sides and the corresponding sides of the parametric cube by means of the

same method with the help of plane functions Φ_μ^μ and let take the resulting mapping as the correspondence between the boundaries; relations (21), (22) specify the boundary conditions everywhere except lines $\{1/2 < y < 1,\ x = 0,\ z = 0\}$ where we define the linear distribution $\xi_2 = 1 - 2y$. As a result we get the coordinate grid depicted on fig. 6.

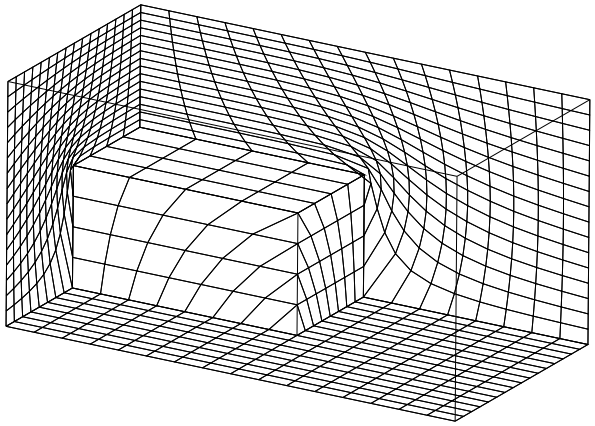

Figure 6: Boundary conditions for coordinate functions

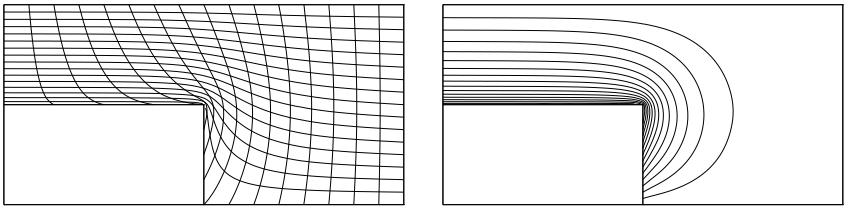

Figure 7: Levels of $\{\xi_1,\ \xi_2\}$ and ξ_3 in section $z = 0.5$

On fig. 7, 8 there are iso-levels of the coordinate functions near singular elements of the boundary, we got these lines as a result of the computations. On fig. 7 on the left there are levels of $\{\xi_1,\ \xi_2\}$, and on the right – levels of ξ_3 on the edge of the trihedral corner in the section $\zeta = 0.5$. We can see the concentration of isolines close to the boundary point which results in the appearance of degenerate hexahedrons in harmonic grid. Fig. 8 contains the distribution of the function $\xi_3(P)$ (left picture) on the circle with radius

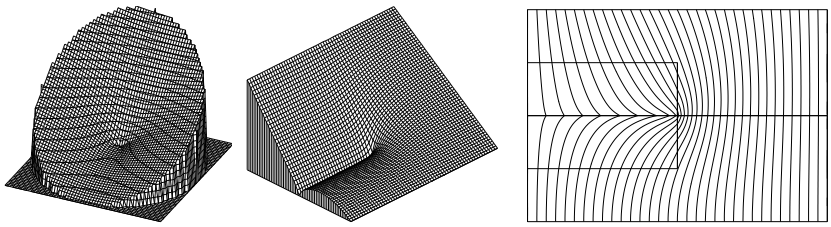

Figure 8: Singularities of harmonic mapping near trihedral corner

$r = 0.25$ that touches the vertices M of the trihedron at the same angle with all axes. Fig. 8 also shows the distribution $\xi_2(P)$ (central picture) on the plane which touches the edge $y = 0.5,\ z = 0.5$ and which is placed at the angle of 45^o with the axes y and z, on the right picture there is the distribution of the levels of $\xi_1(P)$ on the same plane. We can easily observe the singularities of harmonic mapping near the trihedral corner.

7. Some harmonic mappings of doubly-connected domains

There is a need to use harmonic mappings of doubly-connected domains, for example, for the problems in heterogeneous media [12]. On the left of fig. 9 a rectangular cell including the ellipse is represented. This cell can be used for modelling of two-periodical composite material. Such tasks can

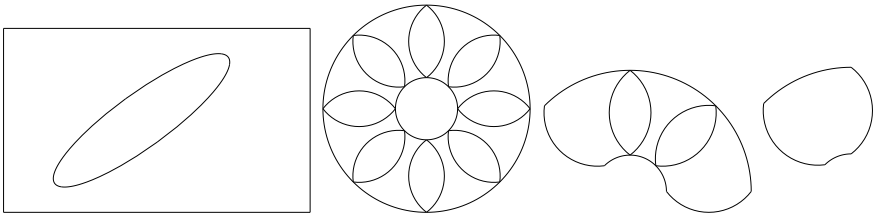

Figure 9: Region with inclusion and the ring subdivision on blocks

also be efficiently solved with the help of block analytic-numeral method because the method is based on coverage $G = \cup \mathcal{B}_k$ of all domain by the simply connected blocks. An example of separation of a ring onto blocks implemented with the help of circles system covering the domain is shown on fig. 9. The doubly-connected 3D domains can be represented as the union $G = \cup \mathcal{B}_k$ in a similar way. For this case the layers $\mathcal{B}_r$, $\mathcal{C}_r$ or $\mathcal{H}_1$ should be chosen as the canonical region.

Let us point out that the domain topologically equivalent to the cylindrical layer can be mapped either onto $\mathcal{C}_r$, or onto $\mathcal{H}_1$ with additional jump condition $\xi_2(P_+) - \xi_2(P_-) = A$ when turning of the inclusion. This condition can be easily reproduced by the block method. However, it is impossible to map the region which includes a 3D area and is topologically equivalent to the sphere layer onto the plane layer $\mathcal{H}_1$; only $\mathcal{B}_r$ can be taken as the canonical region for this mapping.

The ambiguity in specification of (2) provides additional complexity when doing the mapping onto $\mathcal{B}_r$, $\mathcal{C}_r$ or $\mathcal{H}_1$. The mappings from cylindrical layer and sphere layer onto themselves demonstrate this problem:

$$\xi_1 + i\xi_2 = (x+iy)\left[e^{-i\varphi_0} + \frac{1-e^{-i\varphi_0}}{1-r^2}\left(1 - \frac{r^2}{x^2+y^2}\right)\right], \quad \xi_3 = z; \qquad (23)$$

$$\xi_1 = 1 - \frac{\ln\left(x^2+y^2\right)}{2\,\ln r}, \quad \xi_2 = \operatorname{Arctg}\left(\frac{y}{x}\right) - \varphi_0\,\frac{\ln\left(x^2+y^2\right)}{2\,\ln r}, \quad \xi_3 = z. \qquad (24)$$

Formulas (23) specify the harmonic mapping of $\mathcal{C}_r$ onto itself, formulas (24) specify the harmonic mapping of $\mathcal{C}_r$ onto $\mathcal{H}_1$; the inner cylinder is rotated by the angle φ_0; $\operatorname{Arctg}(y/x)$ is the multivalent function which has got a simple

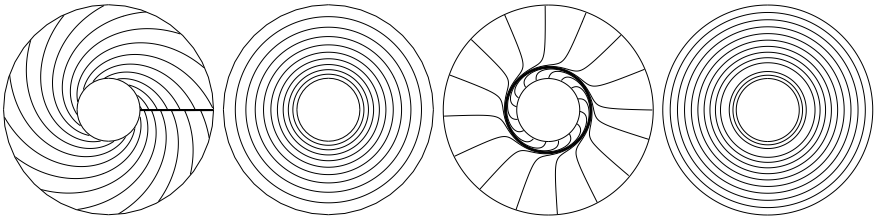

Figure 10: Levels of mappings on $\mathcal{H}_1$ and on $\mathcal{C}_r$

branch $\operatorname{arctg}(y/x)$. On fig. 10 we can see levels of coordinate functions ξ_1, ξ_2 for such mappings. There is an interesting effect for the mapping (23) which is not present for the mapping (24): when the value of the rotation angle increases and when it becomes equal to $\varphi_0 = 2\arccos(r)$ a singular line moves away from the inner cylinder and the mapping stops being one-to-one; this is very well observed on fig. 11 that contains the harmonic grid corresponding to the increasing rotation angle. Similar effect is observed for the mapping of a sphere layer onto itself.

The work was supported by Partner Project – EOARD No 2154.

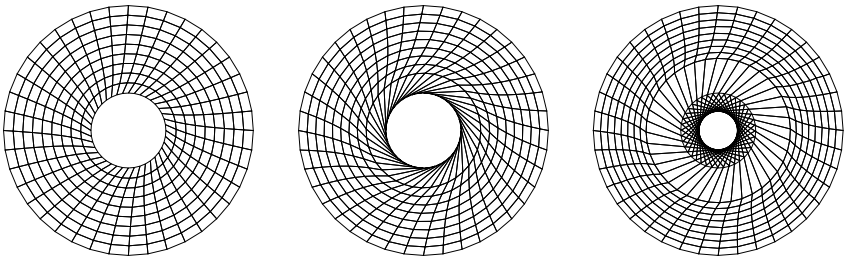

Figure 11: Image of polar grid under increasing rotation angle

8. References

1 Eells, J., Sampson, J.: Harmonic mappings of Riemannian manifolds // Amer. J. Math. Vol. 86 (1964). P.109-160.

2 Harmonic mappings. Handbook of Grid Generation. Ed. by J.F.Thompson, B.K.Soni, N.P.Weatherill; Boca Raton etc: CRC Press, 1998.

3 Vlasov, V.I.: Variation of the mapping function during deformationof a domain // Dokl. Akad. Nauk. SSSR. Vol. 275, No. 6 (1984). P. 1299-1302.

4 Vlasov, V.I., Volkov, D.B.: On properties of domains bounded by circular triangles // Soviet Math. Dokl. Vol. 33, No. 1 (1986). P. 58-61.

5 Vlasov, V.I., Volkov, D.B.: The multipole method for Poisson equation in regions with rounded corners // Comp. Maths Math. Phys. Vol. 35, No. 6 (1995). P. 687-707.

6 Vlasov, V.I., Volkov-Bogorodsky, D.B.: Block multipole method for boundary value problems in complex-shaped domains // ZAMM. Vol. 78, Suppl. 3 (1998). P. 1111-1112.

7 Volkov-Bogorodsky, D.B.: Development block analytical-numerical method for problems in mechanic and acoustic // Proceedings of the conference "Composite materials". M.: IAM RAN, 2000. P. 44-56 (In Russian).

8 Bateman, H., Erdelyi, A.: Higher transcendental functions. Volume 1, 2. New York, Toronto, London: Mc Graw-Hill Book Co., 1953.

9 Tikhonov, A.N., Samarsky, A.A.: Equations of mathematical physics. M.: Nauka, 1966 (In Russian).

10 Vladimirov, V.S.: Equations of mathematical physics. M.: Nauka, 1976 (In Russian).

11 Mikhlin, S.G.: Variational methods in mathematical physics. M.: Nauka, 1970 (In Russian).

12 Bahvalov, N.S., Panasenko, G.P.: Homogenization of processes in periodic media. M.: Nauka, 1984 (In Russian).